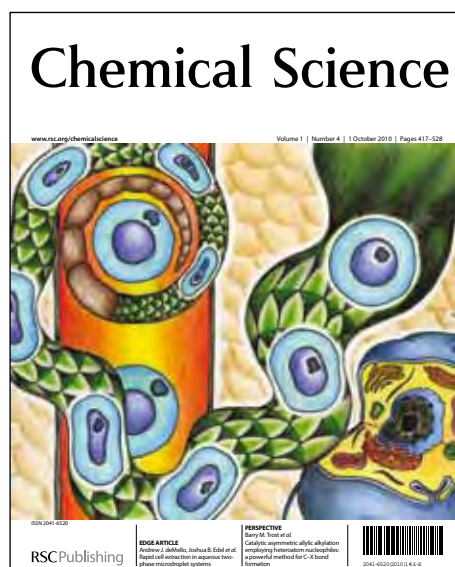


Chemical Science

Accepted Manuscript

This article can be cited before page numbers have been issued, to do this please use: U. Bunz, T. Schwaebel and S. Menning, *Chem. Sci.*, 2013, DOI: 10.1039/C3SC52928B.



This is an *Accepted Manuscript*, which has been through the RSC Publishing peer review process and has been accepted for publication.

Accepted Manuscripts are published online shortly after acceptance, which is prior to technical editing, formatting and proof reading. This free service from RSC Publishing allows authors to make their results available to the community, in citable form, before publication of the edited article. This *Accepted Manuscript* will be replaced by the edited and formatted *Advance Article* as soon as this is available.

To cite this manuscript please use its permanent Digital Object Identifier (DOI®), which is identical for all formats of publication.

More information about *Accepted Manuscripts* can be found in the [Information for Authors](#).

Please note that technical editing may introduce minor changes to the text and/or graphics contained in the manuscript submitted by the author(s) which may alter content, and that the standard [Terms & Conditions](#) and the [ethical guidelines](#) that apply to the journal are still applicable. In no event shall the RSC be held responsible for any errors or omissions in these *Accepted Manuscript* manuscripts or any consequences arising from the use of any information contained in them.

ARTICLE

Photoscapy: Spectroscopic Information from Camera Snapshots?

Cite this: DOI: 10.1039/x0xx00000x

Thimon Schwaebel,^a Sebastian Menning,^a and Uwe H. F. Bunz^{a,*}Received 00th January 2012,
Accepted 00th January 2012

DOI: 10.1039/x0xx00000x

www.rsc.org/

The interconversion of photographic and emission spectroscopic data is described. The approach allows collecting robust color information cheaply and quickly by photography. Photographs of arrays of emissive solutions are obtained in a fraction of a second, containing color information equivalent to that of multiple emission spectra. Critical is the extraction of the color information and comparison to emission spectra of the same array. Calibration of the camera, used as three channel detector is critical. Pseudo color matching functions (not the CIE standard observer), easily measured, are the key. When using RAW data from photographs, the extracted color information (camera specific chromaticity coordinates rg) is unique, but one-to-one correspondence with emission spectroscopic data is not achievable. The rg values are extracted from the emission spectra by multiplication of the spectra with the calibrated, camera pseudo color matching functions. The photograph/spectra relation is unique, as long a single emission line is concerned, true for most practical cases.

Introduction

We herein show the interconversion of spectral and photographic data of solutions of fluorophores by using color coordinates; these define color and allow the direct successful comparison between color information obtained either through spectroscopy or photography.

If one opens a peer-reviewed journal in almost any area of chemistry, there are a score of articles that show snapshots of fluorescent or non-fluorescent dye and dye-analyte solutions.¹ It is obvious that such snapshots are valuable as they often allow direct identification of analytes (eye), but it is less clear, if photographs contain *useful*, extractable, spectroscopic information.

In supramolecular/analytical chemistry a constantly recurring problem is the generation of large amounts of color data.²⁻⁴ These large data sets result, when investigating even small libraries of reactive fluorophores (fluorescent dyes) changing their emission color upon exposure towards chemical or environmental stimuli.⁵ The problem of data acquisition and processing becomes even more serious, if such fluorescent dyes are explored in different solvents and tested against multiple analytes.⁶ Fundamentally, one can perform data acquisition brute force; a plate reader equipped with a fluorimeter takes hundreds of spectra and then compares them for subtle changes in emission wavelength, half peak width and emission intensity. A sophisticated statistical program such as SYSTAT evaluates

the data to discern different analytes binding to the fluorophore. Such an approach is time consuming and not very intuitive.

Often, looking at multiple samples, one can qualitatively discern *all* of the analytes by simple emission color change - in the blink of an eye. Consequently, emission spectroscopy, despite being the gold standard of characterization, may not be the most effective tool when dealing with large amounts of emission data. Digital photography might be a more suitable format to acquire the desired data quickly and efficiently. The central question is, how and if the data acquired by digital photography can be standardized and directly compared to fluorescence spectroscopic data.

Both, analytical chemists and computer graphic designer deal with the interconversion of spectral and photographic information. The transformation of spectral information into photographic data (i.e. color coordinates) has important practical implications for chemists when dealing with large amounts of data, while computer game developers must include diffraction and shadow effects for more sophisticated game graphics using *physical laws*.⁷

Suzuki *et al.* introduced the concept of Digital Color Analysis.⁸ They detected non-luminescence colors and converted absorbance spectra of a lithium ion sensor system with the color matching functions of the *Commission internationale de l'éclairage* (CIE) standard observer (Figure 1) into CIE $L^*a^*b^*$ coordinates (chromaticity) and saw color changes as response to increasing concentrations of lithium ions. We expand this concept to analyze fluorescent colors. We will use Digital Color

Analysis with fluorescence spectra and data from a digital camera to detect and *quickly* identify fluorescent solutions.

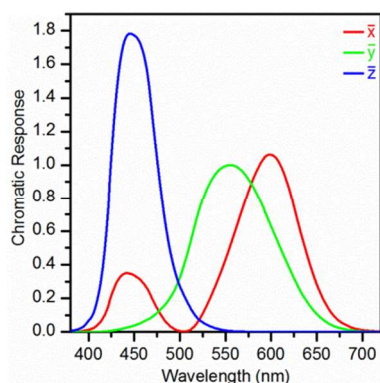


Figure 1. Color matching functions of the CIE standard observer (1931).

We have treated spectroscopic data (from emission spectra) with the standard observer curves (Figure 1) to extract chromaticity coordinates. To compare with values from photographs, we assumed that transformations made by the camera and Adobe Photoshop to convert the light signal into RGB (and therefore chromaticity), employ the CIE standard observer.⁹ Such photo-extracted values unfortunately fall short when comparing them to chromaticity coordinates extracted from spectra of identical solutions. The color matching functions of the camera sensor *are not* the functions of the CIE standard observer and are not available from the manufacturer of our camera, citing corporate secrecy.

We needed to experimentally extract camera depended *pseudo color matching functions* (PCMF) to compare chromaticity coordinates obtained by our camera and the fluorimeter respectively. A digital camera as “spectrometer” seems unorthodox. But it is a detector observing light with a resolution of 5 to 19 mega pixel - each suitable for analysis. Using red, green and blue filters, color information is recorded as intensity of a specific spectral area. Each pixel can be used as a mini detection unit.¹⁰ Multiple samples are recorded simultaneously with one image, making the digital camera an ideal tool for the analysis of even large sensor arrays.

Using calibrated color charts it is possible to calibrate a digital camera for any ambient light. This method is used in photography but it is useless in our case because we record the color of light emitting objects and not spectral reflectance.

Martínez-Verdú *et al.* described a method to determine the PCMFs of a digital camera¹¹ and a procedure to convert the digital camera into an absolute tristimulus colorimeter to identify non-fluorescent colors (spectral reflectance).¹² Sigernes *et al.* introduce a simpler procedure to calibrate a camera for auroral imaging.^{13,14} Using these methods, several PCMFs of commercially available digital camera have been determined.¹⁵

Color Representation

According to Grassmann any color can be described by three or more parameters.¹⁶ These parameters can be colors or attributes

such as saturation, hue and intensity, resulting in different color models. Employing different primary parameters there are several vector color spaces for each color model. Independent of the color model and color space, any color can be transformed mathematically between each of them.

The CIE color model belongs to the color perception of the human eye and encodes all visible colors in a tri-chromatic additive color model. The primary colors (X: imaginary red, Y: imaginary green and Z: imaginary blue) of this model are mathematically constructed and do not correspond to physical colors. There are however additional color value combinations in this color space describing “color” that have no physical meaning.

Color values X, Y and Z of the color space CIE XYZ are easily extracted from *emission spectra* by calculating the integrated product of the emission spectrum of the fluorophore with the color matching functions of the CIE standard observer (Figure 1). The area under the respective curves then represents the numerical color values of the X, Y, and Z coordinates. These XYZ color values are converted into reduced chromaticity coordinates *xy* when normalized spectra instead of absolute spectra are employed, because there is no absolute information about the intensity of the color in the normalized spectra. This procedure can also be employed to a digital camera using PCMFs instead of color matching functions of the standard observer leading to *rg* coordinates instead of *xy*. The color space of the digital camera and that of the human eye (CIE XYZ) are different but it is possible to convert *rg* values to *xy* values if necessary.

To illustrate chromaticity coordinates we focus on the cube of an RGB color space (Figure 2, R: red, G: green and B: blue). Mixing the primary colors RGB in different ratios and values, any color *inside* the cube can be created. If each color is mixed in the same ratio of the primary colors (1:1:1) but with different color values, different shades of grey are constructed on the diagonal connecting black and white. As one can see, the absolute value of the color vector (modulus) defines brightness.

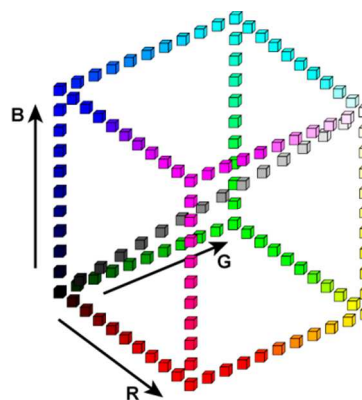


Figure 2. Color space of a RGB color model. All colors inside the cube are mixed by the primary colors R, G, and B. The diagonal connects the achromatic colors, black and white, using the same ration (1:1:1) but different color values of the primary colors.

Chromaticity coordinates are a function of color values and implement a normalization of color information:

$$r = \frac{R}{R + G + B}$$

$$g = \frac{G}{R + G + B}$$

$$b = \frac{B}{R + G + B}$$

As there are normalized values, these encode color without brightness and therefore the equation $1 = r+g+b$ applies. Consequently, any combination of two variables is enough to solve this equation and to describe color. For convenience rg values are selected in style of the CIE coordinates xy .

How are xy and rg values connected conceptually? The chromaticity coordinates xy belong to the color space CIE XYZ with the standard observer color matching function. Any other color matching functions result in a different RGB color space with its own specific rg chromaticity coordinates. Consequently we can also transform emission spectroscopic data into rg coordinates of this specific color space by integration of the spectral features with the PCMFs. In principle any detection device has its own color space and it should be noted by subscript the specific PCMFs. There are mathematical transformations to convert rg coordinates into *device independent* xy coordinates.¹⁸ However, as we only use the PCMF of *our* camera, subscript and transformation is not necessary.

Results and discussion

Determination of pseudo color matching functions. Simple setups (SI; **Setup I, III** and **IV**) record grid diffracted, monochromatic light with a fiber spectrometer and a digital camera (Canon EOS 7D). The monochromatic light obtained from the grating ranged from 390 to 710 nm. From this data, we extracted for the same wavelength both, the spectra of the monochromatic light $L(\lambda)$ (Figure 4, middle) and the normalized RAW counts of the image intensities for each channel k (R, G, B) (left). Data obtained from JPEG pictures cannot be employed, because their RGB color values are not linearly transformed by the camera software and do not obey the formula of image irradiance. We create the PCMFs $S^{(k)}(\lambda)$ for this specific camera (right). Simplified, the recorded image intensities of the three channels R, G and B are divided by the spectra of the monochromatic light (see a detailed procedure in the SI). Independent of the used setup the determined PCMFs are similar (SI; Figure S27; Figure S28). Using an Ulbricht sphere (SI; **Setup I**) is favoured over a screen (SI; **Setup III** and **VI**) because the light is recorded directly and not a reflection. Therefore it is recommended to use an Ulbricht sphere though this is expensive equipment.

The color matching functions of the CIE standard observer (Figure 1) and the PCMFs of the Canon EOS 7D (Figure 4,

right) are not identical. Transforming the rg coordinates of the monochromatic light into the CIE xy chromaticity diagram, we determined the gamut of the Canon EOS 7D (Figure 3).¹⁸ The red dots represent the chromaticity coordinates of the monochromatic light and enclose the color space of the camera. This gamut does not match the gamut of the human eye but the biggest part of the observed color is correctly encoded by the camera. This mismatch results probably from the process of calculating the transformation matrix. There are several methods to determine the transformation matrices¹⁸ and it is important in digital photography to have the correct transformation matrices to capture the correct colors of a scene. But for our purposes we do not have to know the correct transformation matrix, as we adjust the processing of our spectral data. *Using the specific PCMFs of our camera instead of the standard observer color matching functions*, we obtain camera-specific chromaticity coordinates rg values from the emission spectra. We work in the rg chromaticity diagram of our digital camera and *not* in the chromaticity diagram (xy) of the standard observer.

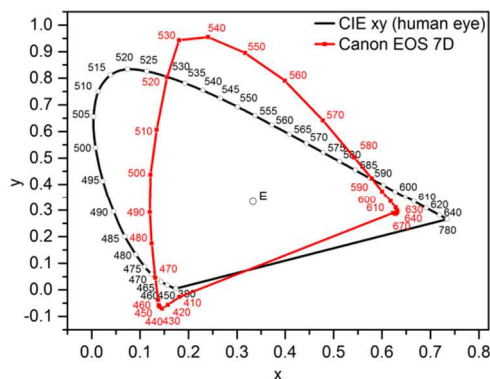


Figure 3. The CIE 1931 color space chromaticity diagram with the gamut of the human eye (black) and with the gamut of our digital camera Canon EOS 7D (red). The red dots represent the chromaticity coordinates of the monochromatic light that was employed here. The attached numbers on the lines represent the wavelength in nm of the corresponding monochromatic light and E the white point.

This calibration is the center piece of this contribution; it allows with optimized parameters of our photographic setup to directly compare rg values from emission spectra with those obtained from photographs. In our hands, for emitted light well visible by the human eye, an exposure time of $t = 1/10$ s, with an f-number of F 2.8, ISO value of 100 and a fixed white balance of 5500 K gives reliable results. *Note that we do not use the camera to take pictures in the traditional sense, instead it acts as a three filter detector.* We tested this detector for three light sources: LEDs, solutions of inorganic quantum dots and solutions of organic fluorescent dyes.

Identification of LEDs. We investigated LEDs with emission colors from blue to red and white, but we could not record the light of the LEDs directly. The high intensity of LEDs overexposed the sensor of the camera so we mounted the different LEDs in position P (SI, **Setup I**) illuminating the integration sphere. We took spectra and photographs of the

emission color at the opening of the Ulbricht sphere (Figure 5, left). With the PCMF in hand we recorded normalized spectra of the LEDs, calculated the chromaticity coordinates rg of their color and then compared these to the photo-extracted rg values

of the same LEDs (Figure 5, right) (see a detailed experimental description in the SI). The match is excellent with a deviation of 0.0018 to 0.0115.

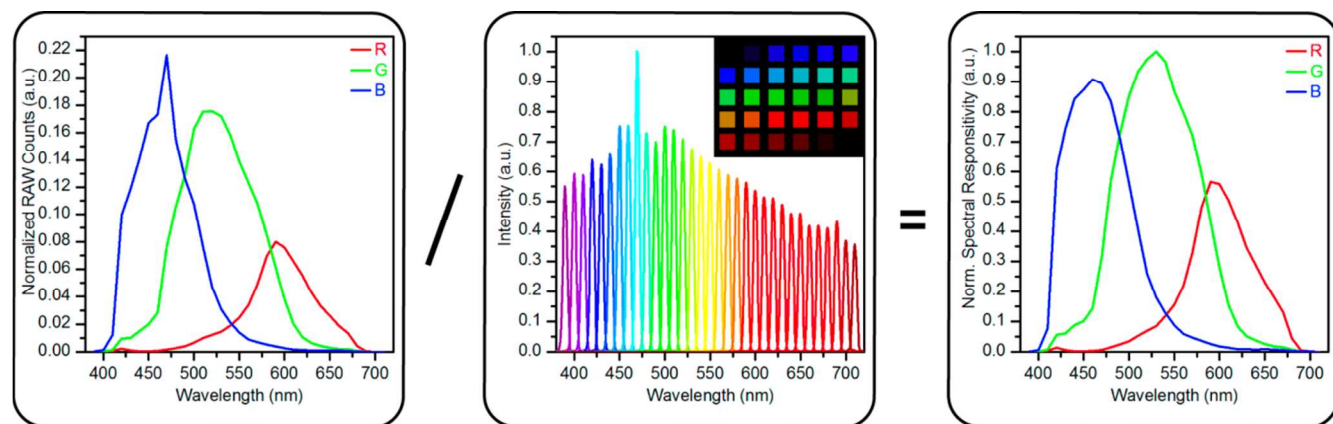


Figure 4. Depiction of calculation of PCMFs of the digital camera Canon EOS 7D (right) using Setup I (SI, Figure S1). Normalized RAW counts of the image intensities of the channel R, G, B (left). Relative monochromatic spectra (middle). The inlet shows the JPEG images of the recorded light from 400 - 690 nm.

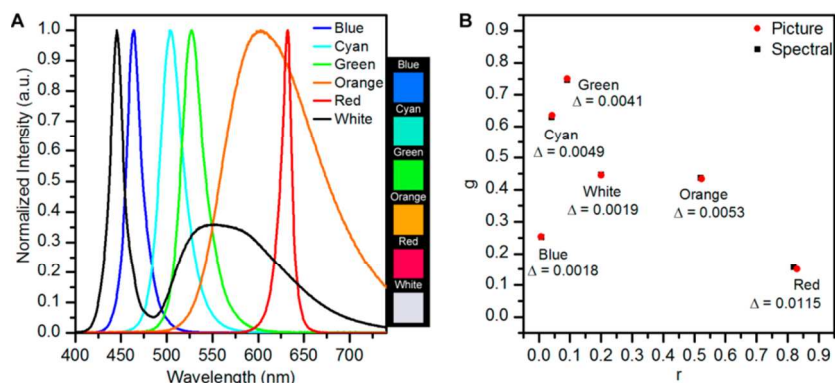


Figure 5. Normalized emission spectra and JPEG photographs of the LEDs (A); comparison of the chromaticity coordinates rg obtained from the spectra (black) and the photography (red) of LEDs placed adjacent to the Ulbricht sphere (SI, Setup I) (B). The deviation Δ is next to each pair.

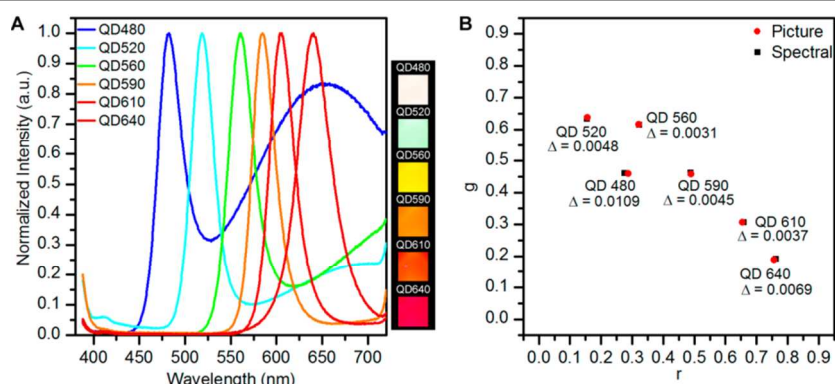


Figure 6. Normalized emission spectra and JPEG photographs of the quantum dot solutions (A); comparison of the chromaticity coordinates rg obtained from the emission spectra (black) and from the photography (red) of CdSe quantum dot solutions in toluene (B). The deviation Δ is next to each pair.

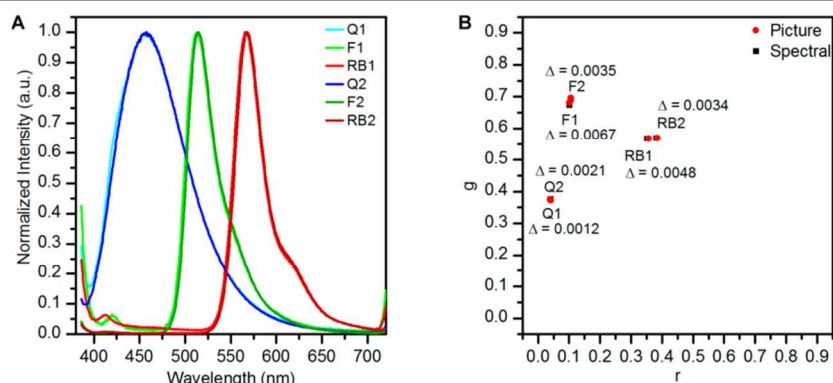


Figure 7. Normalized emission spectra and JPEG photographs of the dye solutions (A); comparison of the chromaticity coordinates rg obtained from the emission spectra (black) and from the photography (red) of solutions of the fluorophores quinine sulfate (Q), rhodamine b (RB), and fluoresceine (F) at two different concentrations (B). The deviation Δ is next to each pair.

Identification of fluorescent solutions of CdSe-quantum dots and solutions of organic dyes. To investigate fluorescent solutions we changed the setup (SI, **Setup II**). A 3 W UV-LED (excitation peak at 370 nm) excited the drum vial. The quantum dot solutions had a concentration of $5 \mu\text{g mL}^{-1}$ (**QD 520**) and $25 \mu\text{g mL}^{-1}$ (**QD480**, **QD560**, **QD590**, **QD610**, **QD640**) in toluene. The quantum dots emitted narrowly with emission maxima at 480, 520, 560, 590, 610 and 640 nm (**QD480**, **QD520**, **QD560**, **QD590**, **QD610** and **QD640**). For **QD480**, **QD520** and **QD560** a second bathochromically shifted emission is observed (Figure 6, left). Despite some handling issues,¹⁹ the match between calculated chromaticity coordinates rg of the emission spectra and the ones recorded with the camera are excellent (deviation 0.0031 - 0.0109; Figure 6, right).

Table 1. List of deviation of data from spectra (spec) and pictures (pic) of organic dye solutions.

Combination	Deviation	Combination	Deviation
Entry 1: Q1 _{spec} - Q1 _{pic}	0.0012	Entry 7: Q1 _{spec} - Q2 _{pic}	0.0023
Entry 2: F1 _{spec} - F1 _{pic}	0.0067	Entry 8: Q2 _{spec} - Q1 _{pic}	0.0030
Entry 3: RB1 _{spec} - RB1 _{pic}	0.0048	Entry 9: F1 _{spec} - F2 _{pic}	0.0223
Entry 4: Q2 _{spec} - Q2 _{pic}	0.0021	Entry 10: F2 _{spec} - F1 _{pic}	0.0124
Entry 5: F2 _{spec} - F2 _{pic}	0.0035	Entry 11: RB1 _{spec} - RB2 _{pic}	0.0326
Entry 6: RB2 _{spec} - RB2 _{pic}	0.0034	Entry 12: RB2 _{spec} - RB1 _{pic}	0.0247

To expand our investigation, we examined fluorescent solutions of quinine (**Q1**; $0.25 \mu\text{M}$ in $0.1 \text{ M H}_2\text{SO}_4$), fluoresceine (**F1**; $0.29 \mu\text{M}$ in 0.1 M NaOH) and rhodamine B (**RB1**; $0.16 \mu\text{M}$ in EtOH) emitting at 450, 520 and 550 nm. There is no problem to identify these when comparing chromaticity coordinates calculated from the spectra and the ones recorded with the digital camera (Figure 7, right). The deviation of photographic

and spectroscopic rg values is small (0.0012 - 0.0067; Table 1; Entry 1 - 3).

We investigated the organic fluorophores at different concentrations (**Q2** $2.5 \mu\text{M}$ in $0.1 \text{ M H}_2\text{SO}_4$; **F2** $2.9 \mu\text{M}$ in 0.1 M NaOH ; **RB2** $1.6 \mu\text{M}$ in EtOH) therefore the shutter speed need to be shortened one-tenths to avoid overexposure of the sensor. Having a small Stokes shift, the emission of smaller wavelength light was reabsorbed, resulting in changed emission spectra, with the emission maximum shifted to the red.²⁰ This change was visible for the normalized emission spectra of fluoresceine and rhodamine B (Figure 7, left). The small changes in emission are detected both in the emission spectra and the chromaticity coordinates rg resulting in two pairs of rg coordinates (Figure 7 right). Deviations between 0.0021 and 0.0035 (Table 1, Entry 4 - 6) make the identification of the solutions with higher concentration better due to higher signal-to-noise ratio.

The large Stokes shift of quinine makes the normalized emission spectra insensitive to changes in concentration. The chromaticity coordinates of either spectrum can be used to compare them with the ones recorded with the camera with excellent results (Table 1, Entry 7 - 8). We cannot cross-compare rg values obtained for fluoresceine or rhodamine B (spectra/photographs) when different concentrations are used (Table 1, Entry 9 - 12).

Conclusions

We have determined pseudo color matching functions (PCMFs) for our digital camera (Canon EOS 7D) and used those to identify fluorescent colors by camera chromaticity coordinates. These rg values are well comparable to rg values extracted from fluorescence spectra of the same solutions, suggesting that a digital camera can act as an rg “spectrometer”. This approach works well for emissive solutions that have one emissive line. We developed a simple experimental setup up using basic mathematical transformations, RAW data from the digital camera and normalized (or relative) fluorescent spectra to perform this feat. Data extraction in the RAW format is

necessary to extract valid color information from photographic data, as JPEG data are nonlinearly transformed by the camera software. Non-reproducible chromaticity coordinates result. Working with RAW data allows calculating chromaticity coordinates rg from normalized emission spectra with the camera specific PCMFs and recording the same coordinates of the light situation with the digital camera.

The knowledge of PCMFs allows extracting *quantitative* color information using digital cameras as a detector, practically repurposing it as an effective rg spectrometer. Chromaticity coordinates rg of digital pictures can now be compared with converted values from libraries of emission spectra employing PCMFs. The applications of such a rg spectrometer could be far ranging and include the analysis of fluorescent test strips for quality control or presence of adulterations in medical drugs etc.. Both, the insignificant price and the large amount of data that can be recorded very quickly make this project attractive and possibly supremely useful.

Acknowledgements

We thank the “Struktur und Innovationsfond des Landes Baden-Württemberg” for the funding of the necessary equipment (fluorimeter, UV-vis spectrometer and camera) and the electricians of the Kirchhoff-Institut Heidelberg and Organisch-Chemischen-Institut Heidelberg for building all necessary LED equipment.

Notes and references

^a Organisch-Chemisches Institut, Ruprecht-Karls-Universität Heidelberg, Im Neuenheimer Feld 270, 69120 Heidelberg, FRG. E-mail uwe.bunz@oci.uni-heidelberg.de.

† Electronic Supplementary Information (ESI) available: Experimental details are provided for the behavior of a digital camera towards image irradiance, as well as step by step tutorials to determine and use pseudo color matching functions.. See DOI: 10.1039/b000000x/

- (a) J. B. Pollock, G. L. Schneider, T. R. Cook, A. S. Davies, P. J. Stang *J. Am. Chem. Soc.*, **2013**, *135*, 13676–13679. (b) Q. A. Best, N. Sattenapally, D. J. Dyer, C. N. Scott, M. E. McCarroll *J. Am. Chem. Soc.*, **2013**, *135*, 13365–13370. (c) C. Reus, S. Weidlich, M. Bolte, H.-W. Lerner, M. Wagner *J. Am. Chem. Soc.*, **2013**, *135*, 12892–12907. (d) J. E. Kwon, S. Park, S. Y. Park *J. Am. Chem. Soc.*, **2013**, *135*, 11239–11246. (e) R. Nishiyabu, P. Anzenbacher, Jr. *J. Am. Chem. Soc.*, **2005**, *127*, 8270–8271. (f) Y. Liu, T. Minami, R. Nishiyabu, Z. Wang, P. Anzenbacher, Jr. *J. Am. Chem. Soc.*, **2013**, *135*, 7705–7712. (g) M. A. Palacios, R. Nishiyabu, M. Marquez, P. Anzenbacher, Jr. *J. Am. Chem. Soc.*, **2007**, *129*, 7538–7544. (h) R. Nishiyabu, M. A. Palacios, W. Dehaen, P. Anzenbacher, Jr. *J. Am. Chem. Soc.*, **2006**, *128*, 11496–11504. (i) D. Aldakov, M. A. Palacios, P. Anzenbacher, Jr. *Chem. Mater.*, **2005**, *17*, 5238–5241. (j) J. A. Marsden, J. J. Miller, L. D. Shirtcliff, M. M. Haley *J. Am. Chem. Soc.*, **2005**, *127*, 2464–2476. (k) E. L. Spitler, J. M. Monson, M. M. Haley *J. Org. Chem.*, **2008**, *73*, 2211–2223. (m) E. L. Spitler, S. P. McClintock, M. M. Haley *J. Org. Chem.*, **2007**, *72*, 6692–6699. (n) E. L. Spitler, L. D. Shirtcliff, M. M. Haley *J. Org. Chem.*, **2007**,

- 72, 86–96. (o) L. Y. Niu, H. Li, L. Feng, Y. S. Guan, Y. Z. Chen, C. F. Duan, L. Z. Wu, Y. F. Guan, C. H. Tung, Q. Z. Yang *Anal. Chim. Acta.*, **2013**, *775*, 93–99. (p) J. C. Er, M. Vendrell, M. K. Tang, D. Zhai, Y.-T. Chang *ACS Comb. Sci.*, **2013**, *15*, 452–457. (q) C. Zhang, D. P. Bailey, K. S. Suslick *J. Agric. Food Chem.*, **2006**, *54*, 4925–4931. (r) B. A. Suslick, L. Feng, K. S. Suslick *Anal. Chem.*, **2010**, *82*, 2067–2073. (s) C. Hertzog-Ronen, E. Borzin, Y. Gerchikov, N. Tessler, Y. Eichen *Chem. Eur. J.*, **2009**, *15*, 10380–10386. (t) O. N. Burchak, L. Mugerli, M. Ostuni, J. J. Lacapère, M. Y. Balakirev *J. Am. Chem. Soc.*, **2011**, *133*, 10058–10061. (u) R. J. Meier, S. Schreml, X. Wang, M. Landthaler, P. Babilas, O. S. Wolfbeis *Angew. Chem. Int. Ed.*, **2011**, *50*, 10893–10896. (v) J. Yao, K. Zhang, H. Zhu, F. Ma, M. Sun, H. Yu, J. Sun, S. Wang *Anal. Chem.*, **2013**, *85*, 6461–6468.
- (a) S. L. Wiskur, H. Ait-Haddou, J. J. Lavigne, E. V. Anslyn *Acc. Chem. Res.* **2001**, *34*, 963–972. (b) J. J. Lavigne, S. Savoy, M. B. Clevenger, J. E. Ritchie, B. McDoniel, S. J. Yoo, E. V. Anslyn, J. T. McDevitt, J. B. Shear, D. Neikirk *J. Am. Chem. Soc.* **1998**, *120*, 6429–6430. (c) T. L. Nelson, C. O'Sullivan, N. T. Greene, M. S. Maynor, J. J. Lavigne *J. Am. Chem. Soc.* **2006**, *128*, 5640–5641. (d) M. S. Maynor, T. L. Nelson, C. O'Sullivan, J. J. Lavigne *Org. Lett.* **2007**, *9*, 3217–3220.
- (a) J. Lim, O. S. Miljanic *Chem. Commun.* **2012**, *48*, 10301–10303. (b) J. Lim, D. Nam, O. S. Miljanic *Chem. Sci.* **2012**, *3*, 559–563.
- (a) N. A. Rakow, K. S. Suslick *Nature*, **2000**, *406*, 710–713. (b) C. J. Musto, K. S. Suslick *Curr. Op. Chem. Biol.* **2010**, *14*, 758–766. (c) K. S. Suslick, N. A. Rakow, A. Sen *Tetrahedron*, **2004**, *60*, 11133–11138.
- (a) P. Montes-Navajas, L. A. Baumes, A. Corma, H. Garcia *Tetrahedron Lett.* **2009**, *50*, 2301–2304. (b) J. Yao, K. Zhang, H. Zhu, F. M. Sun, H. Yu, J. Sun, S. Wang *Anal. Chem.* **2013**, *85*, 6461–6468. (c) T. Eaidkong, R. Mungkarndee, C. Phollookin, G. Tumcharern, M. Sukwattanasinitt, S. Wacharasindhu *J. Mater. Chem.* **2012**, *22*, 5970–5977.
- (a) A. J. Zuccherro, P. L. McGrier, U. H. F. Bunz *Acc. Chem. Res.* **2010**, *43*, 397–408. (b) J. Kumpf, U. H. F. Bunz *Chem. Eur. J.* **2012**, *18*, 8921–8924. (c) P. L. McGrier, K. M. Solntsev, S. Miao, L. M. Tolbert, O. R. Miranda, V. M. Rotello, U. H. F. Bunz *Chem. Eur. J.* **2008**, *14*, 4503–4510. (d) C. Patze, K. Broedner, F. Rominger, O. Trapp, U. H. F. Bunz *Chem. Eur. J.* **2011**, *17*, 13720–13725.
- Y. Sun, F. D. Fracchia, T. W. Calvert, M. S. Drew, *IEEE Computer Graphics* **1999**, *19*, 61–67.
- K. Suzuki, E. Hirayama, T. Sugiyama, K. Yasuda, H. Okabe, D. Citterio *Anal. Chem.* **2002**, *74*, 5766–5773.
- T. Schwaebel, O. Trapp, U. H. F. Bunz *Chem. Sci.* **2013**, *4*, 273–281.
- L. Byrne, J. Barker, G. Pennarun-Thomas, D. Diamond, S. Edwards *Trends in Anal. Chem.* **2000**, *19*, 517–522.
- F. Martínez-Verdú, J. Pujol, P. Capilla *J. Imaging Sci. Technol* **2002**, *46*, 15–25.
- F. Martínez-Verdú, J. Pujol, P. Capilla *J. Imaging Sci. Technol* **2003**, *47*, 279–295.
- F. Sigernes, J. M. Holmes, M. Dyrland, D. A. Lorentzen, T. Svenøe, K. Heia, T. Aso, S. Chernouss, C. S. Deehr *Opt. Express* **2008**, *16*, 15623–15632.

Journal Name

- 14 F. Sigernes, M. Dyrland, N. Peters, D. A. Lorentzen, T. Svenøe, K. Heia, S. Chernouss, C. S. Deehr, M. Kosch *Opt. Express* **2009**, *17*, 20211-20220.
- 15 H. Zhao, R. Kawakami, R. T. Tan, K. Ikeuchi *Meeting on Image Recognition and Understanding* **2009**, 2009, 1.
- 16 H. Grassmann, *Annalen der Physik und Chemie* **1853**, *89*, 69.
- 17 Michael Bass (1995), *Handbooks of Optics Volume I: Fundamentals, Techniques, and Design*, 2nd edition, McGraw-Hill Inc., chapter 26..
- 18 (a) F. Martínez-Verdú, M. J. Luque, P. Capilla, J. Pujol *Color Res. Appl.*, **31**, 399-410. (b) J. Holm *IS&T/SID 14th Color Imaging Conference*, **2006**, Capture Color Analysis Gamuts.
- 19 W. G. J. H. M. Van Sark, P. L. T. M. Frederix, D. J. Van den Heuvel, H. C. Gerritsen, A. A. Bol, J. N. J. van Lingen, C. de Mello Donega, A. Meijerink *J. Phys. Chem. B* **2001**, *105*, 8281-8284.
- 20 Lakowitz, J. R., *Principles of Fluorescence Spectroscopy*, 3rd edition, chapter 2, Springer Verlag, **2006**.

TOC

